

Research article

Haploinsufficient *Bmp4* ocular phenotypes include anterior segment dysgenesis with elevated intraocular pressure

Bo Chang^{†2}, Richard S Smith^{†*1,2}, Maureen Peters⁴, Olga V Savinova², Norman L Hawes², Adriana Zabaleta², Steven Nusinowitz⁶, Janice E Martin^{1,2}, Muriel L Davisson², Constance L Cepko^{1,4}, Brigid LM Hogan^{1,3} and Simon WM John^{*1,2,5}

Address: ¹The Howard Hughes Medical Institute, ²The Jackson Laboratory, Bar Harbor, ME, USA, ³Department of Cell Biology, Vanderbilt University Medical School, Nashville, TN, USA, ⁴Department of Genetics, Harvard Medical School Boston, MA, USA, ⁵Department of Ophthalmology, Tufts University School of medicine, Boston, MA, USA and ⁶Department of Ophthalmology; UCLA Jules Stein Eye Institute, Los Angeles, CA, USA

E-mail: Bo Chang - bchang@jax.org; Richard S Smith* - rss@jax.org; Maureen Peters - maureen_peters@student.hms.harvard.edu; Olga V Savinova - ovs@jax.org; Norman L Hawes - nlh@jax.org; Adriana Zabaleta - zabaleta@jax.org; Steven Nusinowitz - nusinowitz@isei.ucla.edu; Janice E Martin - jemartin@jax.org; Muriel L Davisson - mtd@jax.org; Constance L Cepko - cepko@rascal.med.harvard.edu; Brigid LM Hogan - Brigid.hogan@mcm.vanderbilt.edu; Simon WM John* - swmj@jax.org

*Corresponding authors †Equal contributors

Published: 6 November 2001

Received: 1 October 2001

BMC Genetics 2001, 2:18

Accepted: 6 November 2001

This article is available from: <http://www.biomedcentral.com/1471-2156/2/18>

© 2001 Chang et al; licensee BioMed Central Ltd. Verbatim copying and redistribution of this article are permitted in any medium for any non-commercial purpose, provided this notice is preserved along with the article's original URL. For commercial use, contact info@biomedcentral.com

Abstract

Background: Glaucoma is a blinding disease usually associated with high intraocular pressure (IOP). In some families, abnormal anterior segment development contributes to glaucoma. The genes causing anterior segment dysgenesis and glaucoma in most of these families are not identified and the affected developmental processes are poorly understood. Bone morphogenetic proteins (BMPs) participate in various developmental processes. We tested the importance of *Bmp4* gene dosage for ocular development and developmental glaucoma.

Results: *Bmp4*^{+/-} mice have anterior segment abnormalities including malformed, absent or blocked trabecular meshwork and Schlemm's canal drainage structures. Mice with severe drainage structure abnormalities over 80% or more of their angle's extent have elevated IOP. The penetrance and severity of abnormalities is strongly influenced by genetic background, being most severe on the C57BL/6J background and absent on some other backgrounds. On the C57BL/6J background there is also persistence of the hyaloid vasculature, diminished numbers of inner retinal cells, and absence of the optic nerve.

Conclusions: We demonstrate that heterozygous deficiency of BMP4 results in anterior segment dysgenesis and elevated IOP. The abnormalities are similar to those in human patients with developmental glaucoma. Thus, *BMP4* is a strong candidate to contribute to Axenfeld-Rieger anomaly and other developmental conditions associated with human glaucoma. *BMP4* also participates in posterior segment development and wild-type levels are usually critical for optic nerve development on the C57BL/6J background. *Bmp4*^{+/-} mice are useful for studying various components of ocular development, and may allow identification of strain specific modifiers affecting a variety of ocular phenotypes.

Background

Glaucoma is a leading cause of blindness that involves loss of retinal ganglion cells and degeneration of the optic nerve [1]. Glaucoma is usually associated with high intraocular pressure (IOP) that results from an increased resistance to drainage of the ocular fluid [1]. Developmental disorders of the ocular anterior segment, including Axenfeld-Rieger syndrome, are often associated with elevated IOP and glaucoma [1,2]. The developmental sequence and structure of the human and mouse ocular drainage structures are similar [3], and the same genes are known to cause anterior segment dysgenesis (ASD) in humans and mice. Known genes that cause anterior segment dysgenesis code for developmentally important transcription factors. These genes include *PITX2*, *PITX3*, *PAX6*, *FOXC1* (previously known as FKHL7 and FREAC3), *Foxc2* and *FOXE3* [4–9]. Activity levels for these transcription factors normally associated with diploid gene dosage are important for normal ocular development, with heterozygosity for null mutations in most of these genes causing anterior segment dysgenesis. For *FOXC1* and *PAX6*, both haploinsufficiency and increased gene dosage due to gene duplication result in abnormal ocular development [10–13]. Similarly, a mutation in *PITX2* that results in increased transcriptional transactivation causes ASD [14].

Bone morphogenetic proteins (BMPs) are a large subclass (more than 20 members) of the TGF- β superfamily. Although originally named because of their ability to induce bone and cartilage formation [15], BMPs are involved in many developmental processes, including cell proliferation and differentiation, apoptosis, and intercellular interactions during morphogenesis [16–25]. Members of the bone morphogenetic protein family function in a gene dosage dependent manner during development and participate in ocular development [26–29]. Therefore, mutations that alter the level of BMPs or alter the degree of BMP signaling are candidates to contribute to Axenfeld-Rieger syndrome and other conditions involving anterior segment malformation, elevated IOP, and glaucoma. Interestingly, some BMPs modulate tooth morphogenesis [30] and Axenfeld-Rieger patients present with dental abnormalities.

Bmp2 and *Bmp4* are two members of the BMP family, closely related to *Drosophila dpp* (decapentaplegic). *Bmp4* is expressed in multiple tissues during embryonic development, including the heart, lung, kidney, brain, and eye [19,24]. In the eye, *Bmp4* expression is first identified in the distal optic vesicle and overlying surface ectoderm at the 8–12 somite stage and later in the dorsal portion of the developing optic cup [31]. Lens induction is absent in homozygous *Bmp4* mutants and can be rescued by exogenous BMP4 protein [31].

The effects of decreasing *Bmp4* dosage on anterior and posterior segment development have not been reported. In this study, we analyzed mice heterozygous for a null allele of *Bmp4* (*Bmp4^{tmlBlh}*) [24] to determine if decreased functional gene dosage contributes to ASD and elevated IOP. Heterozygous *Bmp4* mutant mice have a variety of ocular abnormalities including ASD, buphthalmia (enlarged eyes), and elevated IOP. This work functionally demonstrates that BMP4 is a good candidate to cause human ASD and developmental glaucoma.

Results

Bmp4 expression

Eyes of *Bmp4^{lacZneo}* heterozygotes on a mixed background [25] were evaluated for β -galactosidase expression at embryonic ages E14.5, E16.5, new born, postnatal ages P2, P14, and P30 (Figure 1). Expression was found in iris, ciliary body, and retinal pigment epithelium at E14.5 and became more intense after birth. Expression continued at the same level at P30. Expression was also demonstrated in the endothelial cells of conjunctiva, retina, and orbit. Importantly, expression was not present in the developing trabecular meshwork and Schlemm's canal (ocular drainage structures) or in hyaloid vascular endothelial cells. All other studies described in the following sections were carried out on mice with the *Bmp4^{tmlBlh}* targeted mutation [32] (hereafter, *Bmp4^{+/-}*), and are based on *Bmp4^{+/+}* and *Bmp4^{+/-}* mice. Unless otherwise stated, the mice had a C57BL/6J (B6) genetic background.

Anterior segment dysgenesis

Slit lamp examination revealed a variety of anterior segment abnormalities in *Bmp4^{+/-}* but not in *Bmp4^{+/+}* mice (normal littermates) that were 3 to 5 months of age. The specific phenotype varied from mouse to mouse and eye to eye (Figure 2A,B,C). Some affected eyes were relatively normal with only an irregularly shaped pupil. Most commonly, however, there were abnormal iridocorneal attachments (anterior synechiae) of variable extent, large irregularly shaped pupils that were often eccentrically located, and a displaced Schwalbe's line. Several eyes had peripheral corneal thinning while others demonstrated scleralization (opacity) of the peripheral cornea, diffuse corneal haze, or peripheral neovascularization (Figure 2C). A few mice had anterior subcapsular cataracts.

Histological examination focused on the most severely affected B6 background, and confirmed and extended the clinical observations. Abnormalities were only detected in *Bmp4^{+/-}* mice. The severity of lesions varied within individual eyes and between eyes of the same mouse. In most eyes, the iridocorneal angle was abnormal. The iridocorneal angle contains the ocular drainage

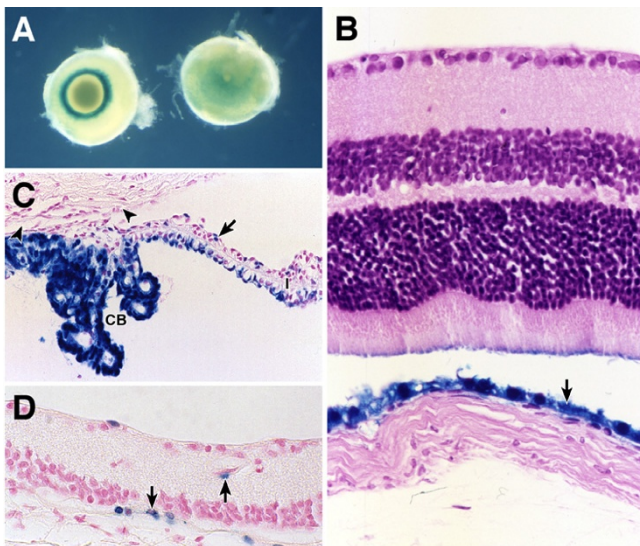


Figure 1
Bmp4 expression assessed by expression of the *LacZ* reporter gene in *Bmp4^{lacZneo}* heterozygotes [25]. All images are from mice of 129/SvEvTac X Black Swiss mixed background that lack obvious haploinsufficient ocular phenotypes. **A.** Newborn mouse, **B-D.** Adult mice. **A.** The left view (anterior of eye) demonstrates intense iris and ciliary body expression. The right view (posterior of eye) shows expression in the retinal pigment epithelium. x 16. **B.** Adult mouse retina. Expression is only evident in the retinal pigment epithelium (arrow). There is some adherence of stain at the tips of the photoreceptors that have become detached from the pigment epithelium during processing. This likely represents expression in the retinal pigment epithelium. H&E/LacZ x 400. **C.** Adult iris and ciliary body. *Bmp4* is predominantly expressed in the epithelia of the iris (I) and ciliary body (CB). A few iris stromal vessels are stained (arrows), but there is no expression in the trabecular meshwork (bounded by arrowheads), x 400. **D.** Isolated staining of retinal vessels (arrows). The outer nuclear layer is absent in this mouse that was homozygous for *Pde6brd*. x 400.

structures (trabecular meshwork and Schlemm's canal) and is located at the junction of the iris and cornea. Abnormalities of the iridocorneal angle included small or absent Schlemm's canal (SC), hypoplastic or absent trabecular meshwork (TM) that appeared compressed and stalled in development, and iris attachments to the peripheral cornea (synechiae. Figure 2D,E,F). Despite the synechiae and abnormal pupils, most *Bmp4^{+/-}* mice had generally normal iris architecture. The iris in some eyes, however, was hypoplastic and malformed (Figure 2F), and occasionally the malformation was extensive involving both iris and ciliary body. The peripheral cornea was often thinner than normal with neovascularization. There was abnormal persistence of the anterior hyaloid

vessels (Figure 2F). Anterior subcapsular and cortical cataracts occurred in most mice.

To investigate the consequences of functionally halving *Bmp4* gene dosage on iridocorneal angle development in more detail, we used transmission electron microscopy. In *Bmp4^{+/+}* mice, the TM consisted of robust trabecular beams with abundant organized collagen and elastic tissue cores that were covered with endothelial-like trabecular cells. SC had a normal appearance and was lined with endothelial cells. In contrast, SC was often absent and the TM had developed abnormally or was absent in *Bmp4^{+/-}* mice. Even in places where the TM was relatively normal, there were fewer trabecular beams and a paucity of extracellular matrix (ECM) components, including organized collagen bundles and elastic tissue. For example, in the posterior trabecular meshwork of wild type mice, there are normally 7–10 trabecular beams [3], but *Bmp4^{+/-}* mice had only 1–2 beams and these beams were nearly devoid of collagen (Figure 2G,H,I,J). Further ECM abnormalities were present in the peripheral cornea where prominent irregularity of the normally regularly arranged collagen bundles explained the peripheral corneal scleralization.

Intraocular pressure

To determine the effects of decreased *Bmp4* gene dosage on intraocular pressure, we compared the IOPs of age- and strain-matched *Bmp4^{+/-}* and *Bmp4^{+/+}* mice. We initially assessed the IOPs of 2 to 5 month old mice. At these ages, 7 out of 17 *Bmp4^{+/-}* heterozygotes had elevated IOP (defined as an IOP greater than two standard deviations above the mean of the *Bmp4^{+/+}* mice). To determine if the incidence of elevated IOP changed with age, we analyzed groups of mice at the ages of 6 to 10 months and 12 to 16 months. The incidence did not change appreciably with 5 out of 10 mice having elevated IOP at 6 to 10 months and 4 out of 9 having elevated IOP at 12 to 16 months (Figure 3). *Bmp4* genotype had a significant effect on IOP (ANOVA, $P < 0.004$) whereas age and sex did not.

Due to the variability in both anterior segment abnormalities and IOP, we reasoned that histological analysis of eyes with high versus normal IOP might provide insight to the extent of abnormalities required to cause elevated IOP. The incidence of drainage structure abnormalities and synechiae deemed severe enough to significantly decrease or prevent aqueous humor drainage was recorded by careful analysis of many sections from different regions around these eyes (see Methods). Our data suggest that IOP is normal even when 50% of the iridocorneal angle around the circumference of the eye is severely abnormal. Furthermore, all four of the studied eyes with high IOP also had severe abnormalities

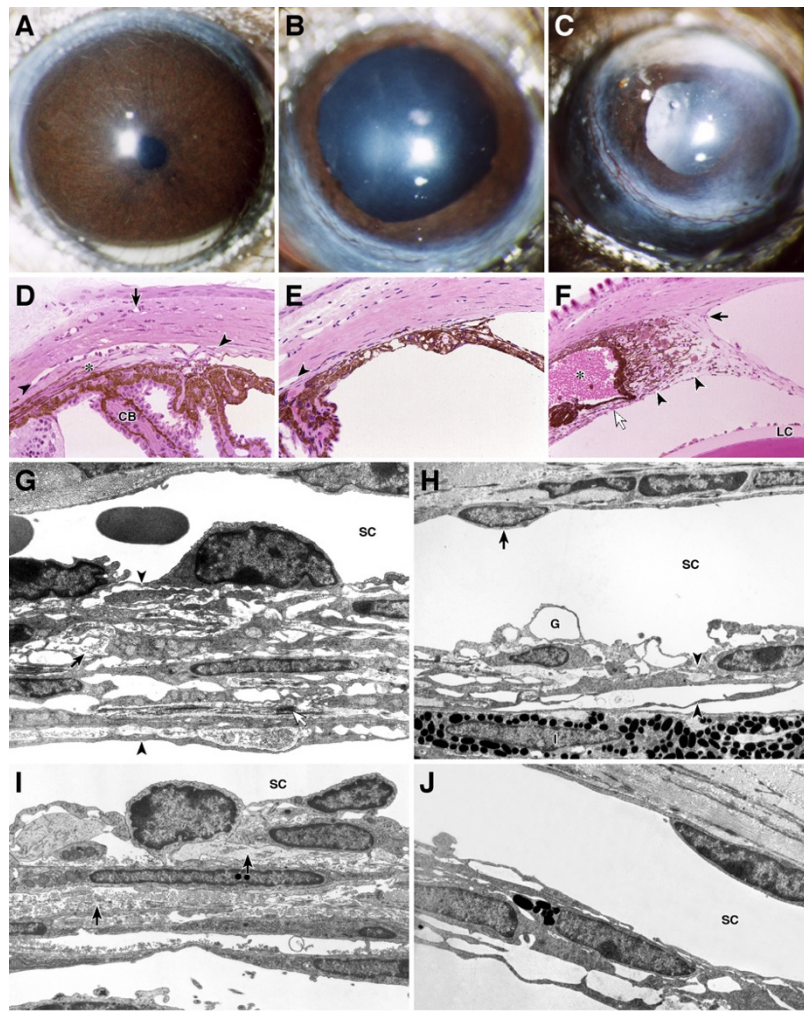


Figure 2

All images are from *Bmp4*^{+/-} heterozygotes on the C57BL/6J background, except for G and I that are from normal mice. **A-C.** Slit-lamp photographs indicate phenotypic variability between individuals, but most eyes are similar to those shown in B and C. **A.** The eye is normal. **B.** There is central corneal haze, an abnormally large and irregular pupil, and an anterior subcapsular and cortical cataract. **C.** The cornea is hazy and the pupil is open and irregularly shaped. There is an anterior subcapsular cataract and inferiorly the peripheral cornea is opaque and vascularized. **D.** The iridocorneal angle is relatively normal at this location with an obvious Schlemm's canal (bounded by arrowheads), trabecular meshwork (asterisk) and ciliary body (CB). The cornea is scarred and vascularized (arrow). This corresponds to the inferior opacification in B. H&E x 200. **E.** SC is abnormally short (arrowhead) and the trabecular meshwork is absent. A broad anterior synechia covers the region where outflow structures are normally located. H&E x 200. **F.** The hypoplastic iris is directly attached to the termination of Descemet's membrane (arrow). SC and the trabecular meshwork are absent. The ciliary body is severely malformed with no ciliary processes (arrowheads). Fibrovascular tissue (white arrow) appears to have drawn pigmented ciliary epithelium posteriorly to form a pseudocyst (asterisk) filled with blood. Persistence of the anterior vascular tunic of the lens is obvious anterior to the lens capsule (LC). H&E x 200. **G.** A wild type C57BL/6J mouse has a normal posterior trabecular meshwork (between arrowheads) and SC. Several layers of trabecular beams are present. Collagen (arrow) and elastic tissue (white arrow) are abundant normal components of the trabecular meshwork. Original magnification x 14,000. **H.** In this *Bmp4*^{+/-} heterozygote, posterior SC is lined by endothelium (arrow) and contains giant vacuoles (G). However, the trabecular meshwork is abnormally thin for this posterior location with only 1–2 trabecular beams (arrowheads) compared to the normal 7–10. Collagen fibers are decreased in number and elastic tissue is absent. In this posterior location, the iris (I) lies close to the meshwork. Original magnification x 12,000. **I.** Anterior trabecular meshwork of normal C57BL/6J mouse. SC is lined by endothelium. Extracellular matrix (arrows) is abundant in both the juxtacanalicular region just below SC and in the trabecular beams. There are 4–5 trabecular beams. Original magnification x 15,000. **J.** The anterior trabecular meshwork of *Bmp4*^{+/-} heterozygote is hypoplastic and both the juxtacanalicular region and trabecular beams contain little extracellular matrix. Original magnification x 15,000.

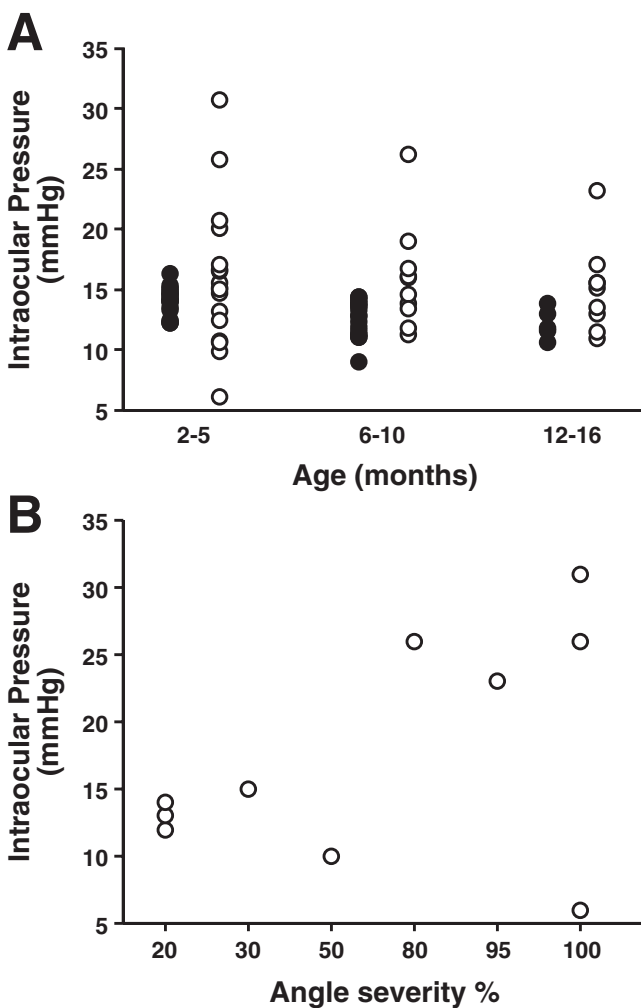


Figure 3
Intraocular pressures in *Bmp4*^{+/+} (filled circles) and *Bmp4*^{+/-} (open circles) mice on the C57BL/6J background. **A.** Some *Bmp4*^{+/-} heterozygotes have elevated IOP at all ages (defined as greater than or equal to 2SD above the mean for normal mice). In the mice that were analyzed at multiple ages, there was no obvious effect of age on IOP elevation. The number of mice analyzed at each age are: at 2 months 19^{+/+}, 17^{+/-}; at 6–10 months 18^{+/+}, 10^{+/-}; at 12–16 months 5^{+/+}, 9^{+/-}. The number of circles sometimes appears different to these values as some mice had identical IOPs. **B.** Histological analysis demonstrated that eyes with high IOP had extensive abnormalities (see Methods), with an estimated 80% or more of the iridocorneal angle circumference being severely malformed. The eye with 100% of analyzed angle locations severely affected and low IOP had a severely malformed ciliary body.

extending over 80% or more of the analyzed sections (Figure 3).

Posterior segment abnormalities

Ophthalmoscopic analysis of *Bmp4*^{+/-} but not *Bmp4*^{+/+} mice revealed irregular white patches in the vitreous and dense vitreous haze in the majority of eyes examined (Figure 4A). The retinal vasculature also was abnormal in *Bmp4*^{+/-} eyes. Fluorescein angiography showed that the main retinal vessels branched close to the optic nerve and were irregularly arranged compared to wild type mice. In addition, there was a dense network of small tortuous vessels throughout the vitreous that leaked fluorescein (Figure 4C). These abnormalities were identified in the youngest (2 to 3 weeks old) and oldest (17 months) mice examined. Severe retinal detachments were observed as early as four months and their incidence increased with age. Although anterior segment cloudiness often made ophthalmoscopy difficult in *Bmp4*^{+/-} heterozygotes, abnormalities of the optic nerve head were frequently present. Combined intraorbital and intracranial dissection of 8 randomly selected mice failed to detect a grossly visible optic nerve in all but one mouse. This mouse had a nerve extending from the right eye but the left nerve was absent. Most dissected eyes had a small white nub of tissue over the scleral foramen.

Histologic analysis confirmed posterior segment abnormalities in *Bmp4*^{+/-} heterozygotes but not in genotypically normal mice. In *Bmp4*^{+/+} mice the hyaloid vessels disappeared around P30, as reported elsewhere [33,34]. In contrast, the hyaloid vessels in *Bmp4*^{+/-} heterozygotes persisted throughout the 17 month period studied and increased in number and size beyond that normally present at birth (Figure 4D,E,F,G). The abnormal vitreous vessels (Figure 4E and 4G) were frequently associated with the formation of adhesions between the retina and lens capsule that exerted traction on the retina resulting in retinal detachment in approximately 25% of the *Bmp4*^{+/-} mice examined and occurred as early as P30. Regression of the hyaloid vasculature is mediated via macrophage-dependent cell death [35]. In the first ten days after birth, macrophages were abundant in the vitreous of *Bmp4*^{+/+} mice, usually localized close to the hyaloid vascular system (Figure 4F). As the hyaloid vessels disappeared the number of macrophages declined. In *Bmp4*^{+/-} mice, macrophages were rarely observed and never identified in the vitreous of mice older than P14.

In agreement with the clinical examinations, optic nerve phenotypes in *Bmp4*^{+/-} mice ranged from normal to absent (Figure 4H,I,J,K). They were often severely abnormal, consisting of loose connective tissue, with absence of neural tissue (Figure 4I,J). Retinal architecture also varied within and between eyes. Although areas of retina were morphologically normal in *Bmp4*^{+/-} mice, the retinal ganglion cell layer was estimated to on average contain approximately 50% the normal number of cells and

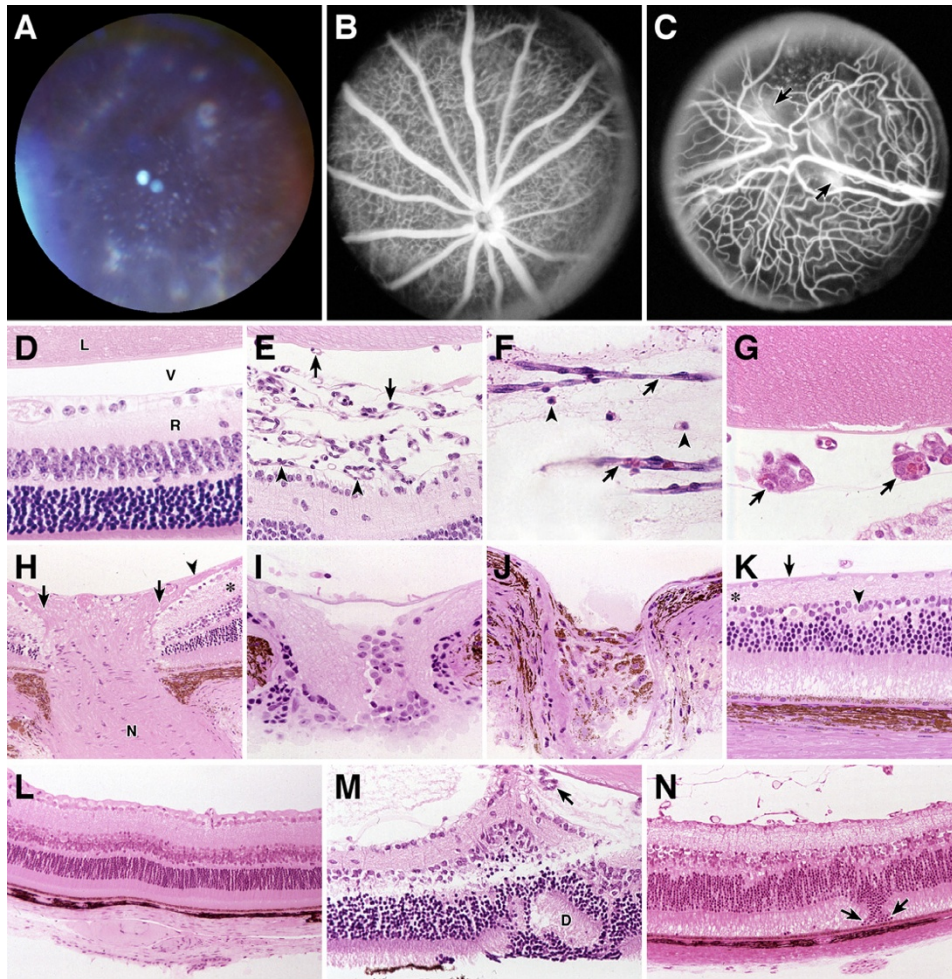


Figure 4

A. Fundus photograph of an adult *Bmp4*^{+/-} mouse. The retinal vessels and optic nerve are obscured by white vitreous opacities of varying size and by diffuse vitreous haze. **B.** Fluorescein angiogram of a wild type C57BL/6J mouse. Both the retinal vessels and the retinal capillary network are sharply defined with the retinal vessels radiating from around the optic nerve. **C.** Fluorescein angiogram of a *Bmp4*^{+/-} mouse. The retinal vasculature is abnormal consisting of large and small vessels that lie on the retinal surface. Abnormal vessels are also present in the vitreous and have areas of leakage (arrows). **D.** Wild type adult retina. All layers of the retina (R) are normal, the vitreous (V) is clear, and the lens (L) normal. H&E x 400. **E.** In this adult *Bmp4*^{+/-} heterozygote, many persistent hyaloid vessels are located directly posterior to the lens (arrows). The hyaloid vessels appear attached to the retinal surface (arrowheads). H&E x 400. **F.** In this wild type P10 mouse (when hyaloid vessel involution begins), macrophages (arrowheads) are arranged parallel to the hyaloid vessels (arrows). H&E x 630. **G.** In this P10 *Bmp4*^{+/-} mouse, macrophages are absent and the hyaloid vessels (arrows) are larger than normal. H&E x 630. **H-I.** Optic nerve phenotypes were variable in adult *Bmp4*^{+/-} heterozygotes. **H.** The optic nerve is normal. The nasal and temporal nerve fibers (arrows) are present beneath the internal limiting membrane (arrowhead) and enter a well-formed optic nerve (N). The peripapillary retina appears normal. H&E x 200. **I.** In this heterozygote, there is no clearly formed optic nerve and no nerve fibers are evident in the scleral canal through which the nerve normally exits the eye. The retina has extended into the canal H&E x 200. **J.** In another heterozygote, the optic nerve is absent and the canal contains pigmented cells and loose connective tissue. H&E x 200. **K-N.** Retinal phenotypes are also variable in *Bmp4*^{+/-} eyes. **K.** Peripapillary retina from a heterozygous eye with a similar optic nerve phenotype to that in I. The internal limiting membrane is present (arrow), but there is no nerve fiber layer. The position marked by an asterisk corresponds to that in H where there is an obvious nerve fiber layer. The inner nuclear layer (arrowhead) is thinner than in H and L. H&E x 200. **L.** In this heterozygote, the retina appears normal (compare to D). H&E x 200. **M.** In this heterozygote, persistent hyaloid vessels are attached to both retina and lens and are exerting vitreous traction (arrow), pulling the retina toward the lens. A focus of retinal dysplasia (D) has disrupted the outer nuclear layer. H&E x 400. **N.** In another *Bmp4*^{+/-} mouse, there is abnormal retinal lamination and a clump of photoreceptor nuclei (arrows) abuts directly onto the retinal pigment epithelium. H&E x 200.

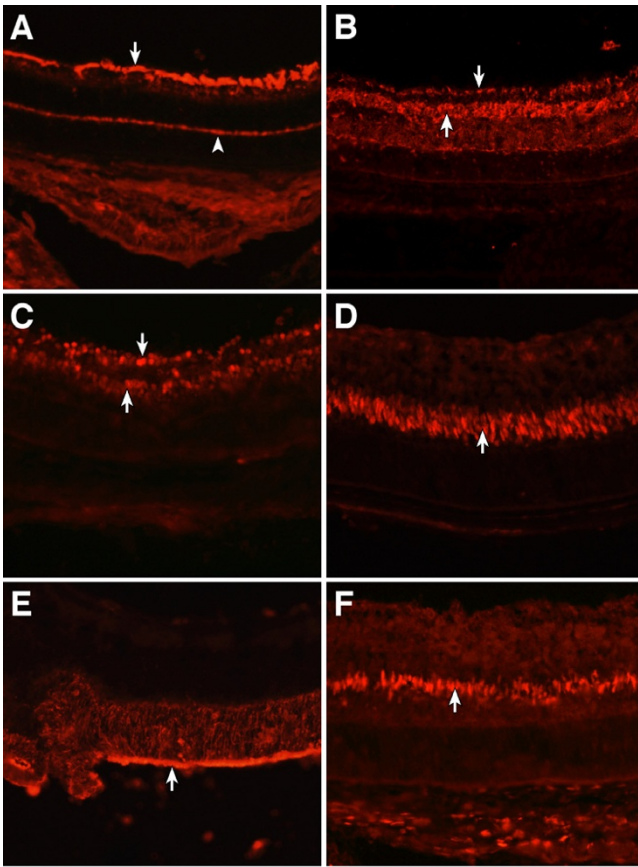


Figure 5
A-F. P7 *Bmp4*^{+/-} retinas treated with a panel of antibodies to retinal markers. **A.** Neurofilament 270 (NF) antibody identifies ganglion cells (arrow) and horizontal cells (arrowhead). **B.** VCI.1 antibody identifies amacrine cells in the inner nuclear layer and displaced amacrine cells in the ganglion cell layer (arrows). **C.** Pax6 antibody identifies progenitors and amacrine cells (arrows). **D.** Chx10 antibody identifies bipolar cells (arrow). **E.** RhoD4 antibody identifies rods (arrow). **F.** Cyclin D3 antibody identifies Muller cells (arrow). **A-F.** x 200.

the inner nuclear layer was unusually thin. The retinal phenotype was variable but present in mice of all analyzed ages including 1 month old. It did not correlate with IOP, being present in both high and normal IOP eyes, and was not obviously worse in old mice than in young mice. In contrast, the photoreceptor layer typically appeared normal though there may have been reduced numbers of cells (Figure 4K). However, there were foci of retinal dysplasia, characterized by rosette formation (Figure 4M). Additionally, there were small areas where photoreceptor nuclei extended externally and were in direct contact with the retinal pigment epithelium (Figure 4N). A panel of retinal cell markers revealed that all major retinal cell types including ganglion cells, horizontal

cells, bipolar cells, amacrine cells, rod and cone photoreceptors, and Muller cells were present in *Bmp4*^{+/-} retinas, and expressed markers of differentiation (Figure 5A,B,C,D,E,F).

Electroretinography

We used full field electroretinography (ERG) to study retinal function in 15 *Bmp4*^{+/-} heterozygotes. Eyes with extensively opaque corneas or obvious cataracts were not used for ERG assessment, and mice with retinal detachments were dropped from the study. There was variability in both severity and age of detectable abnormalities. Compared to normal mice, some *Bmp4*^{+/-} eyes had normal responses even at ages up to 15 months (the oldest age assessed for these eyes). In other mice, both *a*- and *b*- wave amplitude reductions were seen, due in part to poor pupillary dilation. However, a prominent feature of the ERG waveforms to bright flashes when detectable abnormalities were present was the preferential loss of *b*-wave relative to the *a*-wave. It is well established that the *a*- and *b*- wave components of the bright flash ERG in mice reflect the functional state of outer- and inner- retinal cells, respectively. Our observations of greater deficits of the *b*-wave extend our analysis to the entire retina and are consistent with the histologic abnormalities that are more severe in the inner retina.

Effects of genetic background

The penetrance and severity of anterior and posterior segment phenotypes was strongly influenced by genetic background (Table 1). On the B6 background, both the anterior and posterior segment were abnormal in most *Bmp4*^{+/-} mice with over two thirds having bilateral clinical involvement. In contrast, on the C3H.BLiA background, approximately half of the *Bmp4*^{+/-} mice were clinically affected and this was always unilateral. On this background, the abnormalities were typically limited to the anterior segment (involving enlarged pupils and buphthalmos). On other genetic backgrounds, few, if any, heterozygous mice had clinically detectable ocular dysgenesis.

Discussion

Anterior segment dysgenesis

We provide evidence here that a null mutation of *Bmp4* results in dominantly inherited developmental dysgenesis of the anterior segment. The abnormalities affect a variety of anterior segment tissues including the drainage structures of the iridocorneal angle and are similar to those reported in human patients with ASD and glaucoma [36–38]. The absence of detectable *Bmp4* expression in the drainage structures suggests that BMP4 produced by the ciliary body and/or iris may act as a growth and differentiation factor during angle development. The drainage structures were often hypoplastic with little ex-

Table 1:

| Background | Total | Pupil/iris | Cornea | Cataract | Vitreous vessels | Optic nerve |
|--------------|-------|------------|--------|----------|------------------|-------------|
| C57BL/6j | 31/31 | 30/31 | 13/31 | 7/31 | 23/31 | 18/30* |
| CAST/Ei | 1/7 | 0/7 | 0/7 | 1/7 | 0/7 | 0/7 |
| 129/SvEvT ac | 1/12 | 1/12 | 0/12 | 0/12 | 1/12 | 0/12 |
| BALB/cj | 1/15 | 0/15 | 0/15 | 0/15 | 1/15 | 0/15 |
| C3H.BLia | 6/13 | 5/13 | 3/13 | 0/13 | 1/13 | 0/13 |

*Due to corneal opacities and vitreous vessels, the optic nerves were not clearly viewed in all eyes but considering viewable nerves 12 mice appeared normal. In all cases, the numerator indicates the number of mice affected and the denominator indicates the number analyzed. On C57BL/6j, the eyes of 21 mice were bilaterally affected and 10 unilaterally affected. On all other backgrounds the mice were unilaterally affected. For C57BL/6j, another 100 mice were analyzed. Ninety-five of these were affected but the incidence of specific features was not recorded. Pupil and iris abnormalities included irregularly shaped pupils and iris attachments to the cornea. Corneal lesions included scarring and vascularization. Vitreous vessels indicates the abnormal persistence of these vessels. Aberrant optic nerves typically appeared very cupped and colobomatous. More details of specific phenotypes are provided in the text. C57BL/6j were backcross generation N11 or greater, other strains were N2 or greater. For all backgrounds, wild type controls were analyzed but are not included in the table as none were affected.

tracellular matrix. The defects in *Bmp4* mutant mice may involve abnormal cell-cell adhesion, cell migration, and/or delayed or abnormal differentiation of mesenchymal cells in the iridocorneal angle, including decreased production of ECM. All of these processes can be regulated by ECM [39–41] raising the possibility that BMP4 regulates the production and/or organization of ECM, and that the ECM abnormalities lead to or exacerbate the developmental defects. Alternatively, BMP4 may direct expression of cell surface receptors that participate in cell-cell and cell-matrix interactions affecting both cell migration and ECM composition and/or affecting cell fate.

The nature and variability of anterior segment phenotypes of *Bmp4*^{+/-} heterozygotes resemble those we reported in mice with dominant mutations in the forkhead box genes *Foxc1* and *Foxc2* [42]. However, the *Bmp4* haploinsufficient phenotype is typically more severe. The phenotypic variability both between and within the eyes of genetically uniform mice with *Bmp4* or *Foxc* gene mutations indicates that stochastic developmental events are important in determining the phenotypic outcome. The possible nature of these stochastic events was previously discussed [42].

Elevated intraocular pressure is caused by extensive angle dysgenesis

In humans with ASD, the phenotype is variable even between patients with mutations in the same gene, and the severity of clinically observable dysgenesis does not correlate with IOP. The etiology of IOP elevation is not well defined. Different *Bmp4* heterozygotes had high, low or normal IOP. Although *Bmp4*^{+/-} eyes of each IOP class had some degree of drainage structure abnormalities,

only eyes with severe drainage structure abnormalities extending over 80% or greater of the analyzed locations had high IOP. The requirement for extensive iridocorneal angle damage for IOP elevation agrees closely with independent estimates from studies of human patients with angle recession [43,44]. Ocular trauma can damage the iris and drainage structures in the angle in a manner that is clinically obvious since the iris tissue recedes posteriorly from its normal position. Patients in whom the angle recession extends for 240 to 360 degrees of the angle circumference (67 to 100%) frequently develop elevated IOP and glaucoma whereas patients with less extensive damage typically do not have high IOP, although their risk of progressing to glaucoma is increased. The major difference in most *Bmp4*^{+/-} eyes with low IOP was the presence of severe dysgenesis of the ciliary body that was likely to severely decrease aqueous humor production. Less obvious abnormalities in ciliary body tissues may also affect IOP by altering the volume or composition of the aqueous humor produced and possibly by altering the drainage structures in a paracrine fashion [42]. Thus, more subtle metabolic abnormalities in the ciliary body may interact with the iridocorneal angle phenotypic variation and contribute to variability in IOP elevation between human patients.

***Bmp4* affects retinal vascular development and hyaloid vascular involution**

Bmp4^{+/-} heterozygotes have abnormally arranged retinal blood vessels and abnormal persistence of the hyaloid vasculature. In wild type mice, the absolute number of hyaloid vessels actively decreases between P4 and P10 and all vessels disappear by P30. Elimination of the hyaloid vessels proceeds by programmed cell death in both human [45] and mouse eyes [33,35]. Further-

more, this death of endothelial cells and pericytes does not occur in the absence of macrophages. If macrophages are eliminated with toxic liposomes [34] or in transgenic mice expressing diphtheria toxin from a macrophage specific transgene [46], there is persistence of the pupillary and hyaloid vessels. The failure of capillary regression in the liposome-treated mice can be "rescued" by anterior chamber injection of exogenous bone marrow-derived macrophages [34]. In agreement with these findings, we observed that absence of macrophages in the vitreous of *Bmp4*^{+/-} mice is associated with persistence of these vessels. Additional studies are needed to determine how BMP4 affects the presence of the ocular macrophages required for vascular involution and if BMP4 affects the production of trophic factors or affects the macrophages themselves.

BMP4 has important roles in retinal and optic nerve formation

Vertebrate retinal development is an intricate process involving complex pathways that are not completely understood [47–53]. Although our cell marker analysis indicates that all major retinal cell types differentiate, haploinsufficiency of BMP4 results in a variety of retinal abnormalities. The inner retina is the most severely affected with substantially reduced cell numbers in both the retinal ganglion cell layer and inner nuclear layer of nearly all *Bmp4*^{+/-} mice on the B6 genetic background. Although elevated IOP likely results in inner retinal cell death in glaucoma, deficiency of inner retinal cells in *Bmp4*^{+/-} heterozygotes is at least partly a developmental phenomenon. It does not correlate with IOP, being present in both high and normal IOP eyes. Cell numbers are reduced even in eyes of very young mice, and the phenotype is not obviously worse in old mice. Pressure induced cell death may occur, but the wide variability in severity between eyes may have hidden an effect of high IOP on cell survival.

The optic nerve did not develop normally and appeared to completely lack neural tissue in most B6 *Bmp4*^{+/-} mice. The nerve fiber layer, composed of retinal ganglion cell axons was not evident even adjacent to the scleral foramen where it is normally substantially thickened due to axon convergence on the optic nerve. Further experiments are necessary to determine if BMP4 modulates retinal ganglion cell axon sprouting, elongation, targeting or maintenance, or if BMP4 regulates events in optic nerve glia that affect these processes. BMPs have been implicated in neuronal maturation and axonal targeting. Exogenous BMP7 enhances dendrite but not axon growth in embryonic rat sympathetic neurons [54] and hippocampal neurons [55]. Overexpression studies suggest a link between *Bmp4* and axonal targeting of ganglion cells. Ectopic BMP4 can lead to the upregulation of

Tbx5 in the retina, and *Tbx5* misexpression results in altered retinal ganglion cell axon projections to the tectum [56].

In contrast to the inner retinal layers, the photoreceptor layer typically appeared normal. At some locations, however, there was retinal dysplasia or disorganization of photoreceptor position. Retinal dysplasia is characterized by palisading outer retinal cells that surround a central lumen [57]. It occurs in mice with a variety of genetic defects and in some instances is associated with abnormalities of the retinal pigment epithelium [58–62]. Both during development and in adult life, the retinal pigment epithelium is critical to retinal function [63]. BMP2 and 4 may act as negative growth regulators in the retinal pigment epithelium [64]. It is possible that haploinsufficiency of BMP4 in the retinal pigment epithelium may be responsible for focal retinal dysplasia and displacement of photoreceptor nuclei.

Modifiers and candidate genes

As shown here, haploinsufficiency of BMP4 causes a variety of ocular abnormalities that are strongly influenced by strain-specific modifier genes. Identification of the genetic modifiers that alter these phenotypes may provide an important route to understanding the cellular and genetic interactions underlying various developmental processes involving BMP4.

BMPs interact with target cells through a heteromeric complex of type I and type II transmembrane receptors, coupled to an intracellular downstream pathway that includes Smad transcription factors. The activity of this BMP signaling pathway can be modulated *in vivo* by several different mechanisms. For example, in the extracellular environment numerous antagonists can bind to BMPs and inhibit their interaction with receptors (e.g. noggin, chordin, twisted gastrulation), while dominant negative receptor molecules (e.g. Bambi) and inhibitory Smads (e.g. Smad 6 and 7) interfere with signaling at the cellular level [16] [65,66]. These evolutionarily conserved factors work together to precisely modulate the level of BMP signaling activity *in vivo*. The genes encoding these factors are excellent candidates to modify the phenotypes described here and to cause developmental conditions that associate with glaucoma.

Conclusions

Wild-type levels of BMP4 are important for normal development of the anterior and posterior segments. The importance of BMP4 depends on genetic background. The ocular phenotypes of *Bmp4* mutant mice show that *BMP4* is a strong candidate to contribute to Axenfeld-Rieger anomaly and other developmental conditions associated with human glaucoma. These mice provide a

model to study these diseases and various processes of ocular development.

Materials and Methods

Animal husbandry

All experiments were performed in compliance with the ARVO statement for use of animals in ophthalmic and vision research. *Bmp4^{lacZneo}* mice used for expression analysis were bred at Vanderbilt University Medical Center and eyes transferred to The Jackson Laboratory. All other strains were obtained from The Jackson Laboratory (Bar Harbor, ME). Mice were housed in cages containing white pine bedding and covered with polyester filters. The environment was kept at 21°C with a 14 hour light: 10 hour dark cycle. Mice were fed NIH31 (6 % fat) chow *ad libitum*, and their water was acidified to pH 2.8 to 3.2. The mouse colony was monitored for specific pathogens by The Jackson Laboratory's routine surveillance program (see [<http://www.jax.org>] for specific pathogens).

Clinical examinations

Anterior chambers were examined with a slit lamp and photographs were taken using a 40X objective lens. An indirect ophthalmoscope and a 60 or 90 diopter lens was used to visualize the retinas and optic nerves. For this analysis pupils were dilated with a drop of 1% cyclopentolate [67]. Strain B6 has an incidence of a minor notch in the pupil that is clearly distinguishable from the phenotypes described here [42] and was not included as an abnormal phenotype here.

Histological analysis

Eyes were fixed, processed and then embedded in paraffin or Historesin (Leica, Heidelberg, Germany). More than 30 *Bmp4^{+/-}* mice were studied. Paraffin embedded eyes were sagittally sectioned at 5 µm while plastic embedded eyes were sagittally sectioned at 1.5 µm thickness. Iridocorneal angle morphology was interpreted from plastic sections. For this, 24 to 56 sections from each of 3 to 5 different ocular locations (typically more than 100 sections per eye) were collected, stained with hematoxylin and eosin, and analyzed for each eye. The lens was used as a landmark in collecting these sections. Collected regions included temporal and nasal lens peripheries, central lens, and regions on each side of the lens center that were halfway towards the lens periphery. On grading the incidence of severely affected angle locations, the investigator did not know the IOP values for the eyes. The angles of every high quality section were included and angles whose morphology suggested drainage was not possible were rated severe. LacZ reporter gene expression was performed on 2 mice at each age as previously described [68].

Electron microscopy

Mice were euthanized and eyes were immediately enucleated and fixed, with 0.8% paraformaldehyde and 1.2% glutaraldehyde in 0.85 M phosphate buffer pH 7.2 at 4°C. The eyes were fixed for one hour and the anterior segment removed and cut into 1 x 2 mm blocks that included cornea, iris, trabecular meshwork and ciliary body. Fixation was continued at 4°C for 12 hours and the tissues were washed in phosphate buffer and then postfixed with 1% osmium tetroxide, dehydrated and embedded in epon-araldite resin [69]. One micron sections were cut for orientation; thin sections were stained with uranyl acetate and lead citrate [70].

Intraocular pressure

Intraocular pressures were measured as previously described [71–73]. The pressure was recorded for a 1-minute period following stabilization after the microcannula entered the eye. Mice of different genotypes were included in each measurement period, as were C57BL/6J mice. The IOPs of C57BL/6J are very consistent over time and so these animals were interspersed with experimental mice to ensure that calibration had not drifted and that the system was functioning optimally.

Immunohistochemistry

Four eyes each at P3 and P4, and eight eyes from P7 C57BL/6J mice were analyzed. Half of the eyes were from *Bmp4^{+/-}* mice and half were normal littermates. Eyes were fixed overnight in 4% paraformaldehyde, washed twice in PBS, and equilibrated in 30% sucrose and then frozen in OCT. 20 µm cryosections were prepared, dried overnight, and then stained with various antibodies. Slides were blocked in 10% serum and 0.1–0.4% triton for 1–1 1/2 hours. Primary antibodies were diluted in blocking solution and applied for 1–2 hours. The following antibodies and dilutions were utilized: anti-neurofilament 270 (specific to ganglion cells and horizontal cells, 1:100) [74], anti-cyclin D3 (Muller cells, 1:500, Santa Cruz Biotechnology), VC1.1 (amacrine cells, 1:1000, Sigma), anti-Pax6 (ganglion cells, horizontal cells, amacrine cells, and progenitors, 1:300, Convance), RhoD3 (rod photoreceptor cells, 1:250) [75], anti-blue cone opsin, 1:10,000, [76] anti-Chx10 (Bipolar cells, 1:5000; rabbit polyclonal made against a gst fusion protein). Following primary antibody incubation, samples were washed three times with PBS. Cy3 conjugated donkey anti-mouse or anti-rabbit secondary antibodies (1:200, Sigma) in blocking solution were applied for 1 hour. Following secondary antibody incubation, samples were washed with PBS several times. Nuclear staining was achieved using DAPI.

Electroretinography

Full field ERG was assessed using a previously reported protocol [77]. Briefly, following two hours of dark-adaptation, mice were anesthetized by intraperitoneal injection of a Ketamine/xylazine mixture in normal saline. ERGs were recorded from the corneal surface of one eye after pupil dilation (1% atropine sulfate) using a gold loop corneal electrode together with a mouth reference and tail ground electrode. Flashed stimuli were produced with a Grass Photostimulator (PS33 Plus, Grass Instruments, Quincy, MA) affixed to the outside of a highly reflective Ganzfeld dome. Signals were amplified (x 10,000, 1–1,000 Hz, CP511 AC amplifier, Grass Instruments), digitized (PCI-1200, National Instruments, Austin, TX) and computer-analyzed using custom software in a personal computer. Mouse body temperature was maintained at a constant temperature of 38°C.

Abbreviations

IOP, intraocular pressure; B6. C57BL/6J; BMP; bone morphogenetic protein; ASD, anterior segment dysgenesis; ERG, electroretinography.

Acknowledgments

We thank Jennifer Smith and Felicia Farley for help with figures and references, Ron Hurd for assistance with ERG, Lesley Bechtold for help with EM, Norma Buckley for data entry, Amy Snow and Roy Allen for animal care, Tom Gridley and Susan Ackerman for critical reading of the manuscript. Part of this work was supported by The Foundation Fighting Blindness (FFB528172) and core services were subsidized by the National Cancer Institute (CA134196). BLMH and CLC are Investigators, and SWMJ is an Assistant Investigator of the Howard Hughes Medical Institute. Bo Chang and Richard Smith are equal contributors, listed in alphabetical order.

References

- Ritch R, Shields MB, Krupin T: *The Glaucomas, Clinical Science, 2nd edn. St. Louis, MO: Mosby-Year Book; 1996*
- Shields MB: **Developmental glaucomas with associated anomalies.** In: *Textbook of Glaucoma, Third ed. pp. 235–257. Baltimore: Williams & Wilkins; 1992:235–257*
- Smith RS, Zabaleta A, Savinova OV, John SWM: **The mouse anterior chamber angle and trabecular meshwork develop without cell death.** *BMC Dev. Biol* 2001 [<http://www.biomedcentral.com/1471-213X/1/3>]
- Semina EV, Reiter R, Leysens NJ, Alward WL, Small KW, Datson NA, Siegel Bartelt J, Bierke Nelson D, Bitoun P, Zabel BU, Carey JC, Murray JC: **Cloning and characterization of a novel bicoid-related homeobox transcription factor gene, RIEG, involved in Rieger syndrome.** *Nat. Genet* 1996, **14**:392-399
- Semina EV, Ferrell RE, Mintz Hittner HA, Bitoun P, Alward WL, Reiter RS, Funkhauser C, Daack Hirsch S, Murray JC: **A novel homeobox gene PITX3 is mutated in families with autosomal dominant cataracts and ASMD.** *Nat. Genet* 1998, **19**:167-170
- Hanson IM, Fletcher JM, Jordan T, Brown A, Taylor D, Adams RJ, Punnett HH, van Heyningen V: **Mutations at the PAX6 locus are found in heterogeneous anterior segment malformations including Peters' anomaly.** *Nat. Genet* 1994, **6**:168-173
- Nishimura DY, Swiderski RE, Alward WLM, Searby CC, Patil SR, Benner SR, Kanis AB, Gastier JM, Stone EM, Sheffield VC: **The forkhead transcription factor gene FKHL7 is responsible for glaucoma phenotypes which map to 6p25.** *Nat. Genet* 1998, **19**:140-147
- Mears AJ, Jordan T, Mirzayans F, Dubois S, Kume T, Parlee M, Ritch R, Koop B, Kuo WL, Collins C, Marshall J, Gould DB, Pearce W, Carlsson P, Enerback S, Morissette J, Bhattacharya S, Hogan BLM, Raymond V, Walter MA: **Mutations of the forkhead/winged-helix gene, FKHL7, in patients with Axenfeld-Rieger anomaly.** *Am. J. Hum. Genet* 1998, **63**:1316-1328
- Semina EV, Brownell I, Mintz-Hittner HA, Murray JC, Jamrich M: **Mutations in the forkhead transcription factor FOXE3 associated with the anterior segment ocular dysgenesis and cataracts.** *Hum. Mol. Genet* 2001, **10**:231-236
- Nishimura DY, Searby CC, Alward LW, Walton D, Craig JE, Mackey DA, Kawase K, Kanis AB, Patil SR, Stone EM, Sheffield VC: **A Spectrum of FOXC1 Mutations Suggest Gene Dosage as a Mechanism for Developmental Defects of the Anterior Chamber of the Eye.** *Am. J. Hum. Genet* 2001, **68**:364-372
- Schedl A, Ross A, Lee M, Engelkamp D, Rashbass P, van Heyningen V, Hastie ND: **Influence of PAX6 gene dosage on development: overexpression causes severe eye abnormalities.** *Cell* 1996, **86**:71-82
- Aalfs CM, Fantes JA, Wenniger-Prick LJ, Sluifjter S, Hennekam RC, van Heyningen V, Hoovers JM: **Tandem duplication of 11p12-p13 in a child with borderline development delay and eye abnormalities: dose effect of the PAX6 gene product?** *Am. J. Med. Genet* 1997, **73**:267-271
- Glaser T, Jepeal L, Edwards JG, Young SR, Favor J, Maas RL: **PAX6 gene dosage effect in a family with congenital cataracts, aniridia, anophthalmia and central nervous system defects.** *Nat. Genet* 1994, **7**:463-471
- Priston M, Kozlowski K, Gill D, Letwin K, Buys Y, Levin A, Walter MA, Heon E: **Functional analyses of two newly identified PITX2 mutants reveal a novel molecular mechanism for Axenfeld-Rieger syndrome.** *Hum. Mol. Genet* 2001, **10**:1631-1638
- Wozney JM, Rosen V, Celeste AJ, Mitscock LM, Whitters MJ, Kriz RW, Hewick RM, Wang EA: **Novel regulators of bone formation: Molecular clones and activities.** *Science* 1988, **242**:1528-1564
- Mabie PC, Mehler MF, Kessler JA: **Multiple roles of bone morphogenetic protein signaling in the regulation of cortical cell number and phenotype.** *J. Neurosci* 1999, **19**:7077-7088
- Mehler MF, Mabie PC, Zhang D, Kessler JA: **Bone morphogenetic proteins in the nervous system.** *Trends Neurosci* 1997, **20**:309-317
- Hogan BLM: **Morphogenesis.** *Cell* 1999, **96**:225-233
- Hogan BLM: **Bone morphogenetic proteins: Multifunctional regulators of vertebrate development.** *Genes Dev* 1996, **10**:1580-1594
- Graham A, Francis-West P, Brickell P, Lumsden A: **The signaling molecule BMP4 mediates apoptosis in the rhombencephalic neural crest.** *Nature* 1994, **372**:684-686
- Ritter SJ, Davies PJA: **Identification of a transforming growth factor- β 1/Bone morphogenetic protein 4 (TGF- β 1/BMP4) response element within the mouse tissue transglutaminase gene promoter.** *J. Biol. Chem* 1998, **273**:12798-12806
- Marazzi G, Wang Y, Sassoon D: **Msx2 is a transcriptional regulator in the BMP4-mediated programmed cell death pathway.** *Dev. Biol* 1997, **186**:127-138
- Dale L, Jones CM: **BMP signalling in early Xenopus development.** *Bioessays* 1999, **21**:751-760
- Winnier GE, Blessing M, Labosky PA, Hogan BLM: **Bone morphogenetic protein-4 is required for mesoderm formation and patterning in the mouse.** *Genes Dev* 1995, **9**:2105-2116
- Lawson KA, Dunn NR, Roelen B, Zeinstra LM, Davis AM, Wright CV, Korving JP, Hogan BLM: **Bmp4 is required for the generation of primordial germ cells in the mouse embryo.** *Genes Dev* 1999, **13**:424-436
- Dunn NR, Winnier GE, Hargett LK, Schrick JJ, Fogo AB, Hogan BLM: **Haploinsufficient phenotypes in BMP4 heterozygous null mice and modification by mutations in Gli3 and Alx4.** *Dev. Biol* 1997, **188**:235-247
- Luo G, Hofmann C, Bronckers AL, Sohocki M, Bradley A, Karsenty G: **BMP-7 is an inducer of nephrogenesis, and is also required for eye development and skeletal patterning.** *Genes Dev* 1995, **9**:2808-2820
- Furuta Y, Hogan BLM: **BMP4 is essential for lens induction in the mouse embryo.** *Genes Dev* 1998, **12**:3764-3775
- Jena N, Martin-Seisdedos C, McCue P, Croce CM: **BMP7 null mutation in mice: developmental defects in skeleton, kidney, and eye.** *Exp. Cell Res* 1997, **230**:28-37
- Tucker AS, Matthews KL, Sharpe PT: **Transformation of tooth type induced by inhibition of BMP signaling.** *Science* 1998, **282**:1136-1138
- Furuta Y, Hogan BLM: **BMP4 is essential for lens induction in the mouse embryo.** *Genes Dev* 1998, **12**:3764-3775

32. Winnier G, Blessing M, Labosky PA, Hogan BLM: **Bone morphogenetic protein-4 is required for mesoderm formation and patterning in the mouse.** *Genes Dev* 1995, **9**:2105-2116
33. Ito M, Yoshioka M: **Regression of the hyaloid vessels and pupillary membrane of the mouse.** *Anat. Embryol. Berl* 1999, **200**:403-411
34. Diez-Roux G, Lang RA: **Macrophages induce apoptosis in normal cells in vivo.** *Development* 1997, **124**:3633-3638
35. Lang R, Lustig M, Francos F, Sellinger M, Plesken H: **Apoptosis during macrophage-dependent ocular tissue remodelling.** *Development* 1994, **120**:3395-3403
36. Tawara A, Inomata H: **Developmental immaturity of the trabecular meshwork in congenital glaucoma.** *Am. J. Ophthalmol* 1981, **92**:508-525
37. Shields MB, Buckley E, Klintworth GK, Thresher R: **Axenfeld-Rieger syndrome. A spectrum of developmental disorders.** *Surv. Ophthalmol* 1985, **29**:387-409
38. Anderson DR: **The development of the trabecular meshwork and its abnormality in primary infantile glaucoma.** *Trans. Am. Ophthalmol. Soc* 1981, **79**:458-485
39. Adams JC, Watt FM: **Regulation of development and differentiation by the extracellular matrix.** *Development* 1993, **117**:1183-1198
40. Streuli CH, Bissell MJ: **Expression of extracellular matrix components is regulated by substratum.** *J. Cell Bio* 1990, **110**:1405-1415
41. Lin CQ, Bissell MJ: **Multi-faceted regulation of cell differentiation by extracellular matrix.** *FASEB J* 1993, **7**:737-743
42. Smith RS, Zabaleta A, Kume T, Savinova OV, Kidson SH, Martin JE, Nishimura DY, Alward WLM, Hogan BLM, John SWM: **Haploinsufficiency of the transcription factors FOXC1 and FOXC2 results in aberrant ocular development.** *Hum. Mol. Genet* 2000, **9**:1021-1032
43. Kaufman JH, Tolpin DW: **Glaucoma after traumatic angle recession. A ten-year prospective study.** *Am. J. Ophthalmol* 1974, **78**:648-654
44. Alper MG: **Contusion Angle Deformity and Glaucoma.** *Arch. Ophthalmol* 1963, **69**:455-467
45. Zhu M, Madigan MC, Van Driel D, Maslim J, Billson FA, Provis JM, Penfold PL: **The human hyaloid system: Cell death and vascular regression.** *Exp. Eye Res* 2000, **70**:767-776
46. Lang RA, Bishop JM: **Macrophages are required for cell death and tissue remodeling in the developing mouse eye.** *Cell* 1993, **74**:453-462
47. Kageyama R, Isgibashi M, Takebayashi K, Tomita K: **bHLH transcription factors and mammalian neuronal differentiation.** *Int. J. Biochem. Cell Biol* 1997, **29**:1389-1399
48. Brown NL, Kanekar S, Vetter ML, Tucker PK, Gemza DL: **Math5 encodes a murine basic helix-loop-helix transcription factor expressed during early stages of retinal neurogenesis.** *Development* 1998, **125**:4821-4823
49. Morrow EM, Furukawa T, Cepko CL: **Vertebrate photoreceptor cell development and disease.** *Trends Cell Biol* 1998, **8**:353-358
50. Morrow EM, Furukawa T, Lee JE, Cepko CL: **NeuroD regulates multiple functions in the developing neural retina in rodent.** *Development* 1999, **126**:23-36
51. Holme RH, Thomson SJ, Davidson DR: **Ectopic expression of Msx2 in chick retinal pigmented epithelium cultures suggests a role in patterning the optic vesicle.** *Mech. Dev* 2000, **91**:175-187
52. Livesey FJ, Cepko CL: **Vertebrate neural cell-fate determination: lessons from the retina.** *Nat. Rev. Neurosci* 2001, **2**:109-118
53. Dyer MA, Cepko CL: **Regulating proliferation during retinal development.** *Nat. Rev. Neurosci* 2001, **2**:333-342
54. Chandrasekaran V, Zhai Y, Wagner M, Kaplan PL, Napoli JL, Higgins D: **Retinoic acid regulates the morphological development of sympathetic neurons.** *J. Neurobiol* 2000, **42**:383-393
55. Withers GS, Higgins D, Charette M, Banker G: **Bone morphogenetic protein-7 enhances dendritic growth and receptivity to innervation in cultured hippocampal neurons.** *Eur. J. Neurosci* 2000, **12**:106-116
56. Koshiba-Takeuchi K, Takeuchi JK, Matsumoto K, Momose T, Uno K, Hoepker V, Ogura K, Takahashi N, Nakamura H, Yasuda K, Ogura T: **Tbx5 and the retinotectum projection.** *Science* 2000, **287**:134-137
57. Lahav M, Albert DM: **Clinical and histopathologic classification of retinal dysplasia.** *Am. J. Ophthalmol* 1973, **75**:648-667
58. Smith RS, Roderick TH, Sundberg JP: **Micropthalmia and associated abnormalities in inbred black mice.** *Lab. Animal Sci* 1994, **44**:551-560
59. Nakayama K, Ishida N, Shirane M, Inomata A, Inoue T, Shishido N, Horii I, Loh DY: **Mice lacking p27Kip1 display increased body size, multiple organ hyperplasia, retinal dysplasia, and pituitary tumors.** *Cell* 1996, **85**:707-720
60. Grondona JM, Kastner P, Gansmuller A, Decimo D, Chambon P, Mark M: **Retinal dysplasia and degeneration in RARbeta2/RARgamma2 compound mutant mice.** *Development* 1996, **122**:2173-2188
61. Omri B, Blancher C, Neron B, Marty MC, Rutin J, Molina TJ, Pessac B, Crisanti P: **Retinal dysplasia in mice lacking p56lck.** *Oncogene* 1998, **16**:2351-2356
62. Smith RS, Johnson KR, Hawes NL, Harris BS, Sundberg JP, Davisson MT: **Lens epithelial proliferation cataract in segmental trisomy involving mouse chromosomes 4 and 17.** *Mamm. Genome* 1999, **10**:102-106
63. Raymond SM, Jackson J: **The retinal pigmented epithelium is required for development and maintenance of the mouse neural retina.** *Curr. Biol* 1995, **5**:1286-1295
64. Mathura JR, Jafari N, Chang JT, Hackett SF, Wahlin KJ, Della NG, Okamoto N, Zack DJ, Campochiaro P: **Bone morphogenetic proteins-2 and -4: Negative growth regulators in adult retinal pigmented epithelium.** *Invest. Ophthalmol. Vis. Sci* 2000, **41**:592-600
65. Miyazono K: **TGF-β signaling by Smad proteins.** *Cytokine & Growth Factor Rev* 2000, **11**:15-22
66. Nakayama T, Snyder MA, Grewal SS, Tsuneizumi K, Tabata T, Christian JL: **Xenopus Smad8 acts downstream of BMP-4 to modulate its activity during vertebrate embryonic patterning.** *Development* 1998, **125**:857-867
67. Hawes NL, Smith RS, Chang B, Davisson M, Heckenlively JR, John SWM: **Mouse fundus photography and angiography: a catalogue of normal and mutant phenotypes.** *Mol. Vis* 1999, **5**:22-29
68. Hogan B, Beddington R, Costantini F, Lacy E: *Manipulating the Mouse Embryo, Third edn.* Cold Spring Harbor, NY: Cold Spring Harbor Laboratory Press; 1994
69. Smith RS, Rudt LA: **Ultrastructural studies of the blood-aqueous barrier. 2. The barrier to horseradish peroxidase in primates.** *Am. J. Ophthalmol* 1973, **76**:937-947
70. Bechtold LS: **Ultrastructural evaluation of mouse mutations.** In: *Systematic approach to evaluation of mouse mutations* Edited by Sundberg JP, Boggess D. pp. 121-129. Boca Raton: CRC Press; 1999 121-129
71. John SWM, Hageman JR, MacTaggart TE, Peng L, Smithes O: **Intraocular pressure in inbred mouse strains.** *Invest. Ophthalmol. Vis. Sci* 1997, **38**:249-253
72. John SWM, Savinova O: **Intraocular Pressure Measurement in Mice; Technical Aspects.** In: *Systematic Evaluation of the Mouse Eye: Anatomy, Pathology and Biomethods* Edited by Smith RS, John SWM, Nishina PM, Sundberg JP. Chapter 14B. Boca Raton, FL: CRC Press;
73. Savinova OV, Sugiyama F, Martin JE, Tomarev SI, Paigen BJ, Smith RS, John SWM: **Intraocular pressure in genetically distinct mice: an update and strain survey.** *BMC Genet* 2001, **2**: [http://www.biomedcentral.com/1471-2156/1472/1412]
74. Carden MJ, Trojanowski JQ, Schlaepfer WW, Lee VM-Y: **Two-stage expression of neurofilament polypeptides during rat neurogenesis with early establishment of adult phosphorylation patterns.** *J. Neurosci* 1987, **7**:3489-3504
75. Molday RS: **Monoclonal antibodies to rhodopsin and other proteins of rod outer segments.** *Prog. Ret. Eye Res* 1989, **8**:173-209
76. Chiu MI, Nathans J: **A sequence upstream of the mouse blue visual pigment gene direct blue cone-specific transgene expression in mouse retinas.** *Vis. Neurosci* 1994, **11**:773-780
77. Hawes NL, Chang B, Hageman GS, Nusinowitz S, Nishina PM, Schneider BS, Smith RS, Roderick TH, Davisson MT, Heckenlively JR: **Retinal degeneration 6 (rd6): a new mouse model for human retinitis punctata albescens.** *Invest. Ophthalmol. Vis. Sci* 2000, **41**:3149-3157